Background Rejection in the Milagro Gamma Ray Observatory

C. Sinnis for the Milagro Collaboration

Los Alamos National Laboratory

Abstract. Recent advances in TeV gamma ray astronomy are a result of the ability to differentiate between extensive air showers generated by gamma rays and hadronic cosmic rays. Air Cherenkov telescopes have developed and perfected the "imaging" technique over the past several decades, yet until now no method of background rejection has been successfully used in air shower arrays to detect a source of TeV gamma rays. The development of such a technique is necessary to improve the sensitivity of air shower arrays. We report on a method to differentiate hadronic air showers from gamma ray induced air showers in the Milagro gamma ray observatory. The technique is used to observe the Crab nebula at high significance (4.8σ).

1 Introduction

Ground-based gamma ray astronomy was developed in the 1950's. Yet it was not until the late 1980's that the first source of TeV gamma rays was convincingly observed with a ground-based instrument. The innovation that changed the field was the development of a method to distinguish air showers induced by gamma rays and those induced by hadrons (protons and heavier nuclei), the so-called "imaging" technique . The imaging technique categorizes air showers by the shape and orientation of the Cherenkov light pool as observed in the image plane of an air Cherenkov telescope (Hillas 1985). This technique was used by the Whipple experiment to detect TeV gamma ray emission from the Crab nebula, the first detected source of TeV photons. Since the initial discovery of the Crab at least 5 other sources of TeV gamma rays have been detected (Hoffman *et al.* 1999, Ong 1998, Weekes 2000). Despite the recent success of imaging air Cherenkov telescopes, they have several limitations. Since they are optical instruments they can only observe the sky on clear, dark (moonless) nights (the typical duty cycle of these instruments is between 5 and 10%), and they can only ob-

serve a small fraction of the sky at any one time (of order 4×10^{-3} sr). In contrast, a detector that detects the particles in the air shower that reach the ground, known as an extensive air shower (EAS) array, can operate 24 hours/day, and can simultaneously view the entire overhead sky. Past efforts to distinguish hadronic and gamma ray induced air showers in EAS arrays have relied on the identification of muons. At energies above 100 TeV the CASA and CYGNUS arrays used shielded detectors to identify muons present in hadronic air showers. While the CASA array achieved very high levels of background rejection (rejecting 94% of the cosmic ray background above 115 TeV, and 99.93% of the background above 1175 TeV, while retaining over 72% of the gamma ray signal), no signals were observed in their data (Borione *et al.* 1997). It is generally believed that the absence of sources at these high energies is due to the absorption of high-energy photons by the cosmic background radiation and the steeply falling spectra of astrophysical sources. The Milagro detector is sensitive to much lower energy primary photons ($\approx$500 GeV) and can therefore see sources at much greater distances (redshift $\approx$0.1). Here we report on the development of a technique to reject the hadronic background in Milagro. We demonstrate the efficacy of the technique with a detection of the Crab nebula and discuss possible improvements in the technique.

2 The Milagro Detector

The Milagro TeV gamma ray observatory is described in detail elsewhere in these proceedings (Sullivan *et al.* 2001). Milagro has 723 photomultiplier tubes (PMTs) submerged in a 6-million gallon water reservoir. The detector is located at the Fenton Hill site of Los Alamos National Laboratory, about 35 miles west of Los Alamos, NM, at an altitude of 8600' (750 g/cm^2). The reservoir measures 80m x 60m x 8m (depth) and is covered by a light-tight barrier. The PMTs are secured to a grid of sand-filled PVC sitting on the bottom of the reservoir by a Kevlar string. The PMTs are arranged

in two layers, both on a 2.8m x 2.8m grid. The top layer of 450 PMTs (submerged under 1.35 meters of water) is used primarily to reconstruct the direction of the air shower. By measuring the relative arrival time of the air shower across the array the direction of the primary cosmic ray can be reconstructed with an accuracy of roughly 0.75°. The bottom layer of 273 PMTs (submerged under 6 meters of water) is used primarily to discriminate between gamma ray initiated air showers and hadronic air showers.

2.1 Identification and Rejection of Hadronic Events

It is well known that EAS induced by hadronic cosmic rays contain many more muons (from pion decay) and hadrons than EAS induced by gamma rays of comparable energy. In Milagro, the top 6 meters of water effectively absorb the electromagnetic component of the air showers and we identify hadronic events by looking for bright, compact clusters of light in the bottom layer. Using Monte Carlo simulations we estimate that 79% of all proton showers that trigger Milagro contain a muon and/or a hadron that enters the pond, while only 6% of gamma ray induced air showers contain a muon and/or a hadron that enters the pond. The trigger threshold in the simulation was set to 50 PMTs, the nominal hardware trigger requirement in Milagro.

The parameter used to differentiate hadronic showers is

$$C = \frac{NB_2}{MaxB} \equiv Compactness \qquad (1)$$

where NB_2 is the number of PMTs in the bottom layer with more than 2 photo-electrons (PEs) and $MaxB$ is the maximum number of PEs in any PMT in the bottom layer. Small bright clumps on the bottom will give small values of compactness, while showers that uniformly illuminate the bottom with small hits will give large values of compactness. Figure 1 shows the compactness distributions for Monte Carlo proton showers, Monte Carlo gamma showers, and for data. One sees a clear difference between Monte Carlo gamma ray showers and proton showers. Overall the data matches the Monte Carlo proton distribution reasonably well. Beyond a value of $C \approx 2.5$ one can see a discrepancy between the data and the Monte Carlo proton showers. This discrepancy is due to problems in the pulse height calibration of the detector and is being corrected (see the appendix).

If all events with $C \leq 2.5$ are removed (identified as hadronic), we should retain 54% of the gamma ray events and only 9% of the proton events. This results in an improvement in sensitivity of 1.8. This is often referred to as the Q factor of the cut.

We should note that even for events where no muons or hadrons enter the pond there is an observable difference between air showers induced by hadrons and those induced by gamma rays. Using the same cut on the compactness parameter ($C \leq 2.5$) the Monte Carlo predicts a Q factor of 1.2 for these events (retaining 54% of gamma ray events and 20% of proton events). Examination of the electromagnetic particles that strike the pond shows that they tend to be more energetic
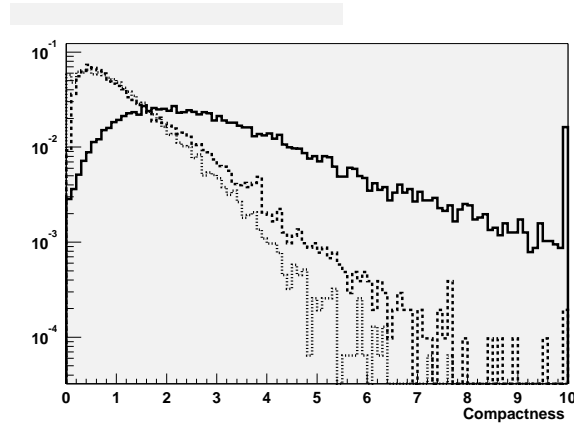

Fig. 1. The compactness distribution for Monte Carlo gamma rays (solid line) Monte Carlo protons (dashed line) and data (dotted line).

and more clumped in hadronic showers than in gamma ray induced showers.

2.1.1 Energy Dependence of Compactness Cut

When analyzing astronomical signals it is important to understand the energy dependence of the instrument. In particular this includes the energy response of any cut performed upon the data. An ideal cut would have an efficiency for signal events that is independent of the energy of the primary gamma ray. In practice such uniformity of response may be difficult to achieve. In Figure 2 we show the efficiency of the compactness cut as a function of primary gamma ray energy. The cut reaches 50% efficiency at ~1.5 TeV. This is below the median energy for gamma ray showers ($E^{-2.4}$ spectrum) that trigger Milagro and get reconstructed into a 2.1° square bin around the source (3.5 TeV). After the compactness cut is applied the median energy rises to 4.7 TeV. Note that the compactness cut is relatively uniform for proton events, while it is a relatively strong function of energy for gamma rays. For a source with a spectral index similar to that of the Crab nebula the energy dependence of the compactness cut does not contribute to the improvement in the significance of the signal (since it preferentially removes the lower energy gamma rays).

3 Application to the Crab Nebula

As a test of the background rejection method we apply it to a search for TeV gamma rays from the Crab nebula. The Crab nebula was first detected at TeV energies in 1989 (Weekes *et al. 1989*). Since that time it has become the standard reference of TeV gamma ray astronomy. With a steady flux of $3.2 \times 10^{-7}(E/TeV)^{-2.49}$ m^{-2}s^{-1}TeV^{-1} (Hillas *et al.*, 1998) it is useful for cross calibrating the sensitivity of different instruments.

The dataset begins on June 8, 1999 and ends on April 24, 2001. Because of detector down time and periods of running
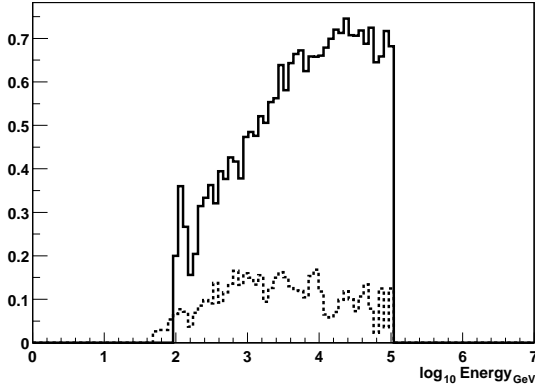
Fig. 2. The energy dependence of the compactness cut. The fraction of gamma ray events (solid line) and proton events (dashed line) retained is shown as a function of energy.

at a lower rate (this data includes the time period when the detector first began taking data and was operating in an engineering mode) the effective exposure of this time interval is roughly 1.35 year of running in our current mode. During this interval we accumulated 50 billion events. The results of the Crab analysis are given in Table 3. We give the results for the raw data and for the data after the compactness cut has been applied. From these results we see a realized Q factor of 4.8. Although somewhat larger than the predicted value, there is a large error on the observed ratio $(4.8 \pm 1.0/1.0 \pm 1.0)$, driven by the 1σ uncertainty in the denominator. The observed excess with no cuts is smaller than the 2.7σ predicted by the Monte Carlo simulations, while there is excellent agreement with the Monte Carlo prediction of 5σ after the compactness cut. The compactness cut removes 91% of the data, consistent with the Monte Carlo prediction of 90% rejection. A clear signal with a significance of 4.8σ is observed with the compactness cut. Since this data was obtained we have improved the pulse height calibration (see Appendix A) of the detector and we expect the details of the result to change. Updated results will be presented at the conference. Figure 3 shows a map of the statistical significance of the excesses in the region around the Crab nebula. At each point we plot the significance of any excess (or deficit) in a 2.1 degree square bin, centered on the bin position. The bin size used is shown as a circle in the figure. The Crab is at the center of the sample bin shown. The left-hand plot shows the significance before the application of the background rejection. The plot on the right shows the significance after the requirement $C > 2.5$ has been applied to the data.

4 Future Improvements

The algorithm described above is quite simple, depending only on the ratio of two quantities, independent of the event size or other characteristics. Monte Carlo simulations indi-

cate that this simple ratio is not independent of other measured quantities in Milagro. Compactness for both gamma rays and protons is a function of the number of PMTs in the bottom layer with more than two PEs. For example, on small events with only a few PMTs illuminated in the bottom layer the compactness parameter may be quite small even if the pulse height in the brightest PMT in the bottom layer is below 8 PE. While these events would be rejected as hadronic events, Monte Carlo simulations indicate that they are most certainly gamma ray events. Similarly for very large events with the core on the pond, gamma ray showers will be mistaken for hadronic events. However, a hadronic core deposits much more energy in the pond than does an electromagnetic core. By examining the full two-dimensional space of $MaxB$ vs. NB_2 we should be able to improve the background rejection in Milagro. Using the Monte Carlo we derive the probability that a gamma ray or proton event will fall at a given point in this space. We use the MARS algorithm developed by J. Freidman (Freidman 1999) to fit these probability densities to a set of spline basis functions. For each point in this space we calculate the ratio of the probability for a gamma ray and a proton to fall at that point in the space (P_γ/P_{proton}). We then find the distribution of P_γ/P_{proton} for all gamma ray and proton events. The optimal value of P_γ/P_{proton} at which to cut the data is determined by maximizing the signal to noise level $(F_\gamma/\sqrt{F_{proton}}$, where F is the fraction of events retained). By excluding all events with $\ln(P_\gamma/P_{proton}) < 2.0$ we remove 88% of the simulated proton events and retain 68% of the gamma ray events, for a predicted quality factor of 2.2 a 20% improvement over the simple compactness cut. An analysis of the Crab data with this cut yields similar results (4.8σ) to the simple compactness cut, consistent with the expected improvement.

5 Conclusions

The bottom layer of Milagro is a coarse imaging calorimeter and can be used to measure the distribution of energy deposited in Milagro. Hadronic cosmic rays generate air showers with penetrating particles that deposit localized clumps of energy in the Milagro detector. We have developed a simple and fast algorithm to differentiate air showers induced by hadronic cosmic rays from those induced by gamma rays. This simple cut based on a compactness parameter improves the sensitivity of Milagro by a factor of 1.8. We have used this cut to observe TeV gamma ray emission from the Crab nebula. This is the first demonstration of the ability of an EAS array to reject hadrons and enhance the significance of an observation of a source of TeV gamma rays. We are currently investigating more sophisticated techniques that utilize more information to improve our background rejection capabilities. As Milagro is a new and unique type of instrument, we are only beginning to understand its response to cosmic rays and gamma rays. As our understanding of this new instrument improves we expect to further improve the sensitivity of Milagro.

Data Selection	ON Source	OFF Source	Excess	Significance
All Data	8,749,562	8,746,621	2941	1.0 σ
Compactness > 2.5	787,503	783,059	4444	4.8 σ

Table 1. Observed excess from the Crab nebula, using all the data and data after the background rejection is applied.
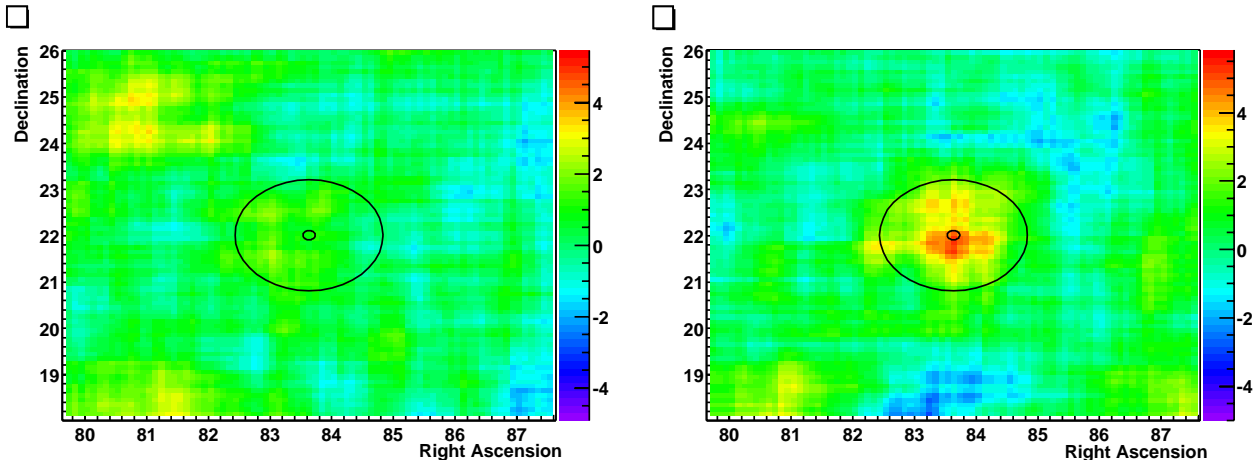

Fig. 3. Significance map of the region around the Crab nebula. The plot on the left shows the significance of all the data (no cut on the compactness). The plot on the right shows the significance after the compactness cut (C>2.5) is imposed on the data. The large circle represents the integration area used in the signal search. The small circle indicates the position of the Crab nebula.

Appendix A Pulse Height Calibration of Milagro

Milagro uses the time-over-threshold (TOT) technique for measuring the pulse height at each PMT. For an exponential pulse one expects the following relationship between TOT and pulse height measured in PEs: $PE = \alpha e^{TOT/\beta}$. where β is the shaping time of the electronics and α is a gain dependent normalization. Thus, the error in the measured pulse height is exponentially dependent upon the error in the measurement of the TOT. In Milagro there can be a significant amount of late light within the detector (due to large angle particles, light reflected from the cover, and scattered light), resulting in large errors in the measurement of TOT. We have minimized this effect by implementing two thresholds on every electronic channel. The first threshold is set at ≈0.25 PEs and the second to ≈6 PEs. Since late light tends to be in the single PE range the higher threshold is relatively immune to mis-measurements of the pulse height, until up to large values of pulse height. Near threshold the TOT technique has a resolution of ≈8% (see Atkins *et al.* 2000).

The initial pulse-height calibration of Milagro used the TOT from the low threshold discriminator up to pulse heights of 15-30 PEs. The late light in the detector causes these measurents to have relatively poor resolution ≈20%. The distribution is asymmetric, with the error typically being to measure a pulse height larger than the true pulse height.

The background rejection technique described in this paper is inherently sensitive to such errors for two reasons: 1) The pulse height range of 8-20 PE is the range of pulse heights that a muon produces in the bottom layer and 2) By selecting the PMT with the maximum value, one is most likely to select the PMT that mismeasured the pulse height. We have recently developed a method that allows us to utilize the laser calibration system to obtain reliable pulse-height calibrations for small values of the high threshold TOT, corresponding to 6-10 PEs. This will significantly improve the pulse-height resolution in this critical region.

References

Atkins, R. *et al.*, NIM A, **449**, p 478, 2000.
Borione, A., et al., Phys Rev D, **55**, p 1714, 1997.
Freidman, J. H., Annals of Statistics, **19**, Issue 1, p 1, 1999.
Hillas, A.M., Proc. 19th ICRC (La Jolla), **3**, 445, 1985.
Hillas, A.M., *et al.*, Astrophys. J., **503**, p 744, 1998.
Hoffman, C. M., Sinnis, C., Fleury, P., and Punch, M., Rev Mod Phys, Vol. 71, No. 4, p 897. 1999
Ong, R., Phys. Rep., **305**, p 13, 1998.
Sullivan, G., *at al.*, these proceedings, 2001.
Weekes, T. C., *et al.*, ApJ, **342**, 379, 1989.
Weekes, T. C., Physica Scripta, **T85**, p 195, 2000